Preliminary Experimental Investigation of a Pulsed Dye Laser at Grazing Incidence.

Diploma paper

Stellan Trappe

Lund Report on Atomic Physics, LRAP-111,
Lund, Mars 1990.

Preliminary Experimental Investigation of a Pulsed Dye Laser at Grazing Incidence.

0 Introduction. 3

1 Laser theory.

1.1 The principles of the laser. 5

1.2 The Laser cavity. 7

1.3 Coherence. 11

1.4 Pumping the laser. 12

1.5 Laser types. 12

2 Gratings and Fabry-Perot interferometers.

2.1 The diffraction grating. 15

2.2 The plane Fabry-Perot interferometer. 17

2.3 The confocal Fabry-Perot interferometer. 20

2.4 The Fringes. 21

2.5 Spectral resolving power. 23

2.6 Light gathering power. 24

2.7 The design of the confocal Fabry-Perot interferometer. 27

3 The Hänsch Laser.

3.1 Introduction. 30

3.2 The Hänsch design. 30

4 The first, grazing incidence, pulsed dye, lasers.

4.1 Why develop the Hänsch laser? 33

4.2 Gratings at grazing incidence. 33

5 Some developments of the pulsed dye laser at grazing-incidence.

5.1 Laser cavity with two gratings. 37

5.2 Gratings at grazing incidence combined with a Fabry-Perot etalon. 39

6 The Littman concept.

6.1 Introduction. 42

6.2 The geometry of the Littman Cavity. 42

6.3 Homogeneously broadened bands. 45

7 Development and applications of the Littman cavity.

7.1 Developments of the Littman laser. 46

7.2 Short pulse generator. 46

7.3 The Littman laser with a Ti:sapphire as active medium. 48

8 Experiments with the Littman cavity.

8.1 The experimental arrangement. 50

8.2 The alignment. 52

8.3 Experiments. 54

R References 60

A Appendix.

A.1 The angular dispersion of the combination grating mirror. 62

A.2 The Littman cavity, technical data. 62

1 Laser theory.

1.1 The principles of the laser.

The remarkable properties of the laser arise from stimulated emission. The ways an atom can change its state are : absorption, stimulated and spontaneous emission. Absorption is the process which transfers the energy of a photon to an atom or molecule, which is thus excited to a higher state. When the atom returns to a lower state by the emission of a photon without any external interaction, the process is called spontaneous emission. Stimulated emission on the other hand is the emission from an excited species induced by the interaction between the species and a photon, where the energy of the photon must equal the energy difference between the upper and lower energy level in the species. The process results in two photons in absolute coherence.

In 1916 Einstein showed, by developing an expression for the energy density of radiation;

$$E(\omega) = \frac{A_{21}/B_{21}}{B_{12}/B_{21}\,[\exp(h\nu/kT)-1]} \qquad 1.1.1$$

a connection between the transition probabilities, A_{21}, the probability of spontaneous emission, B_{12}, the probability of absorption and B_{21}, that of stimulated emission. A comparison with Planck's radiation law reveals;

$$B_{12} = B_{21} \qquad 1.1.2$$

and

$$\frac{A_{21}}{B_{21}} = \frac{h\nu}{\pi^2 c^3}. \qquad 1.1.3$$

The probabilities of stimulated emission and absorption are equal. The ratio between the probabilities of stimulated and spontaneous emission is determined by ν, which is the frequency difference between the atomic energy levels. Large values of ν, favour spontaneous emission.

To make use of the stimulated emission, excited atoms must exist in sufficient numbers. In ensembles of atoms in thermal equilibrium with the environment, the vast majority of atoms are found to be in the

ground state, implying that the probability of obtaining stimulated emission is very small. In order to have an ensemble of atoms to act as a laser the majority of atoms must be in the excited state and must stay there long enough to give rise to an intensive beam. The life time of an excited state is determined by the nature of the transition. The life time of a state that can decay via an allowed transition is very short, about 10^{-12} seconds, but the life time of a state decaying via a forbidden transition may be of the order of 10^{-6} seconds or more. The laser light is not emitted at one single frequency but contains several adjacent frequencies. This line width is quantum mechanically a result of Heisenberg's uncertainty principle. According to this theory a transition with a narrow line width is associated with long-lived atomic levels and, conversely, a transition with a broad line width is associated with short-lived levels. However, to build up an inverted population the laser requires long lived levels and will thus emit light with narrow line widths. The observed widths, however, are not so sharp. This effect, at least for gas and dye lasers, is explained by Doppler and pressure broadening. The light from the atoms in the active medium possess equal broadening when it is caused by pressure, but the Doppler shift affects the atoms according to their condition of motion. Thus when all atoms in an active medium have equal broadening, the broadening is said to be homogeneous, otherwise it is inhomogeneous.

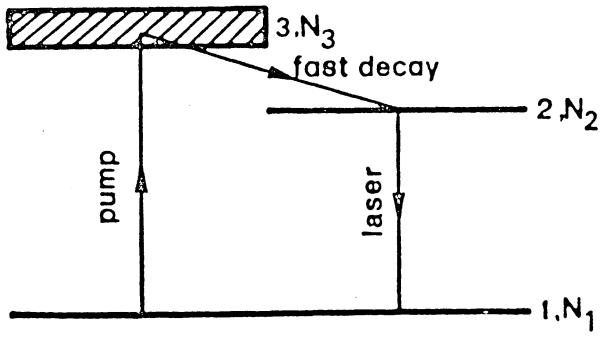

Fig 1.1.1 The three level laser [17].

The state used is usually populated through intermediate states and de-populated to the ground state via these states, as it is difficult to get an inverted population with its ground state as the lowest state. Depending on the number of levels used, two types of laser are distinguished, the rare, three-level laser and the more common, four-

level laser as seen in Figs 1.1.1 and 1.2.1.

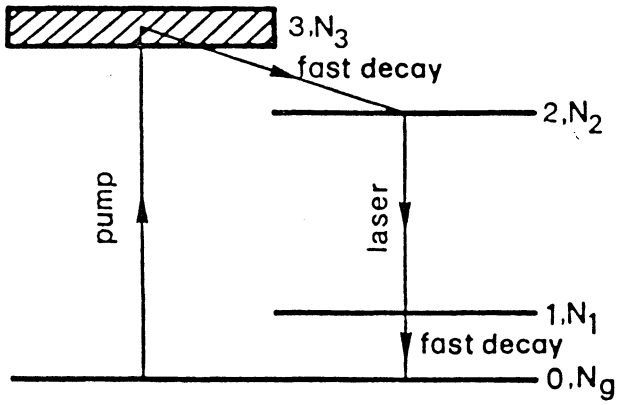

Fig 1.1.2 The four level laser [17].

In an ensemble of excited atoms the introduction of a photon with an energy equal to that of the lasing transition will start an avalanche of photons. To obtain the highest possible yield the active medium is shaped with one dimension far greater than the others, if possible. As an amplifier the active medium has a very low signal to noise ratio. However, with a positive feedback it will act as a light generator with high light intensity.

1.2 The laser cavity.

As a feedback element an optical resonator is used, in it simplest form consisting of two plane paralell mirrors. The light intensity is built up by photons travelling back and forth between the mirrors and through the active medium where stimulated emission creates more photons, the process continuing until the inverted population is lost. If the process is to continue, energy must be supplied to maintain the inverted population. One of the mirrors, which is not fully reflecting, is used as an output coupler. In a perfect laser the losses would only be the output. Unfortunately this is not the case and the losses will occur as a result of, among other things, imperfect mirrors and diffraction. As a measure of the quality of the cavity a Q-value is introduced, defining the quality of the resonant cavity;

$$Q = \frac{\omega_c}{\Delta\omega_c} \qquad 1.2.1$$

where ω_c is the cavity frequency and $\Delta\omega_c$ the band width of the cavity. Q is also expressed by

$$Q \approx 2\pi \frac{L}{\lambda} \cdot \frac{1}{\gamma} \qquad 1.2.2$$

where L is the cavity length and γ expresses the losses of the cavity. Q is proportional to the ratio between the number of standing waves and the losses. A low Q value represents great losses and a large band width, while a high Q value implies low losses and a narrow band width. γ is defined by

$$\gamma = \gamma_i + \frac{1}{2}(\gamma_1 + \gamma_2). \qquad 1.2.3$$

The γ_1 and γ_2 represent losses in the mirrors per single pass and are related to transmission losses, $T_1$and T_2,in each mirror by;

$$\gamma_1 = -\ln(\ 1 - T_1) \qquad 1.2.4$$

and similarly other mirror. Absorption in the mirrors is denoted by a and other losses due to diffraction, diffusion and so on are represented by T_i and the corresponding losses, γ_i, in each single pass are represented by;

$$\gamma_i = -(\ \ln(\ 1 - a\ ) + \ln(\ 1 - T_i)). \qquad 1.2.5$$

The fundamental principle of the laser cavity is that of constructive interference, that is, the length of the cavity is adjusted to create standing waves. The mathematical expression of this condition is

$$l = n\frac{\lambda}{2}, \qquad 1.2.6$$

where n is a positive integer. Usually the lenght of the cavity is

several orders of magnitude greater than the wavelength of the laser, implying that the condition above is satisfied by several pairs (n, λ). This set of pairs represents the modes of the cavity theoretically possible, and the cardinal number of this set is indeed very large. However, the observed number of modes is very much smaller. In a laser the mode structure is determined by two properties of the active medium, its gain profile and its threshold energy. The gain profile is determined by the gain of the active medium as a function of the frequency of light. As an example consider a gas as the active medium of a laser. Due to the movements of the atoms or molecules of the gas, the transitions are broadened by the Doppler shift. This will allow a certain spread of frequencies around the transition frequency. This spread is greater than the natural line width. The threshold intensity is simply the intensity needed to equal the losses of the cavity.

The cavity modes can be described as an electromagnetic configuration whose electric field can be written as

$$\mathbf{E}(\mathbf{r},t) = E_0\mathbf{u}(\mathbf{r}) \exp[(-t/2\tau_c) + i\omega t], \qquad 1.2.7$$

τ_c is the photon decay time of the cavity and is the decay time of the square of the electrical field amplitude. The line width of a mode, $\Delta\omega$, is determined by the cavity life-time through;

$$\Delta\omega = \frac{1}{\tau_c}. \qquad 1.2.8$$

There is also a connection between the cavity life time and cavity losses, γ, since;

$$\tau_c = \frac{L}{c\gamma}. \qquad 1.2.9$$

If the light in the cavity manages to make several round trips, the number of modes will decrease, as the modes near the top of the gain profile will be amplified at the expense of the others. A resonant mode is determined by two factors; ω, the resonant frequency and Q, which in this context is defined by

$$Q = \frac{\omega W}{P_d} \qquad 1.2.10$$

where W is the energy stored in the resonator and P_d is the rate of dissipation [19]. Using the line width of the resonator, $\Delta\omega$, the quality factor may also be expressed as 1.2.1, thus

$$\Delta\omega = \frac{\omega}{Q} \qquad 1.2.11$$

The higher the value of Q, the lower is the energy dissipation and the narrower is the line width.

A laser can be represented as an assemblage of atoms and a resonant cavity with many available resonant frequencies. The atomic system will be characterized by a centre frequency, ω_a ,and a line width, $\Delta\omega$, while the resonant cavity is represented by its resonant frequencies; ω_1, ω_2,..,ω_n and corresponding quality factors; Q_1, Q_2,...,Q_n. The cavity modes obtain their energy from the atomic system and dissipate it through incomplete refection and diffraction or by the escape of radiation to the sides if the modes are not axial. As energy is pumped into the atomic system, atoms will be excited progressively until the level of inverted population is reached at which stimulated emission starts. At this point energy is distributed to the different cavity modes. For those resonant modes which have frequencies near the centre of the atomic resonance, the driving force will be largest. Modes with the highest Q and resonant frequencies near ω_a will be provided with more energy than the others, thus increasing their Q's and making them grow faster. Consequently, modes with increasing Q's will increase their growth rate, but, as the energy supply is the same for all modes in the resonant cavity, the most energetic will gain at the expense of the less energetic until all the radiant energy is concentrated in a few modes. The favoured modes are characterized by being near the centre ω_a which has the highest Q value and where the supply of quanta is greatest.

A laser operating in several modes is said to be running in multi-mode. To obtain light with an extremely short line width, a laser running in single mode has to be used. The most common way to obtain single mode operation is to place a Fabry-Perot etalon in the cavity. The purpose of this device is to select one of the modes and suppress all the others,

and the free spectral range of the etalon has to be chosen accordingly. However, the line width of the laser light might be broadened by mechanical impact i.e. oscillations or mechanical shocks, so that the components have to be mounted on a very stable frame. A servo-system that compensates for any change in the cavity length may also be added.

Besides longitudinal modes the laser may also be oscillating in transverse modes. They are marked by TEM_{mnp}, where m denotes the number of modes in the x-direction, n the modes in the y-direction and p the number of longitudinal modes, (usually omitted). The fundamental mode, denoted TEM_{00}, is circularly symmetric and has a Gaussian intensity distribution. To obtain this mode, circular apertures are inserted in the cavity, the diameters of the apertures being adjusted to the light distribution of a TEM_{00} mode.

1.3 Coherence.

One of the most characteristic properties of laser light is its coherence, that is, the light is emitted in long wave trains with a certain relation between the phases of different parts of the train. The coherence is a consequence of the stimulated emission in which the emitted photon has the same direction as the stimulating photon and is in phase with it. An increment of time (the coherence time Δt) is associated with the length of the wave train, which is connected to the line width $\Delta\nu$ of the laser transition by;

$$\Delta\nu \approx \frac{1}{\Delta t} . \qquad 1.3.1$$

From a quantum mechanial point of view, the uncertainty in the time taken by a given transition implies a certain spread of frequency, which, in turn, affects the length of the wave train. In order to lase, light with narrow line widths is thus associated with long wave trains but the line width of the light from a black body is very broad, and thus has very short wave trains.

The coherence is divided into two categories, the time coherence and the spatial coherence. The time coherence states the possibility to make

predictions about the phase and the amplitude of the light from a certain observation of the phase and the amplitude of the light wave at a later time. A spatial coherence is said to exist if there is a fixed phase difference between distant points. The existence of one kind of coherence does not necessarily imply the existence of the other.

Another property of laser light is that it is highly collimated. The angle of diffraction, Θ_D is expressed by

$$\Theta_D = \beta \frac{\lambda}{D} \qquad 1.3.2$$

where $\beta \approx 1$ for a spatially coherent wave but greater than 1 for a non-spatially coherent wave and D is the diameter of the laser beam. Θ_D is of the order mrad.

1.4 Pumping the laser.

To achieve and maintain an inversion population in the active medium, energy must be supplied. Many ways of supplying energy have been developed over the years, the most common being electrical pumping for gas- and semi-conductor lasers and optical pumping for dye- and solid material-lasers. Optical pumping can be achieved either by pumping with a flashing light or with a laser. Gas lasers are usually pumped by electrical discharges as the narrow absorption bands of gases do not make pumping by flashing light very efficient, due to the broad-banded emission of the flash lamps.

1.5 Laser types.

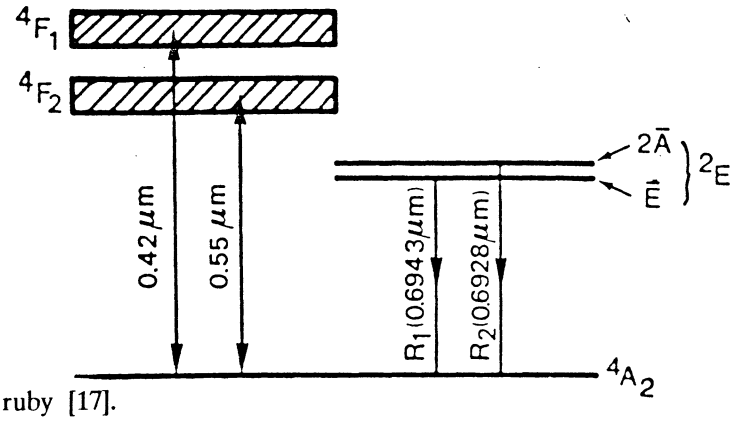

Fig. 1.5.1 Energy levels of ruby [17].

Many different types of lasers have been developed but in this work only crystal-, gas- and dye-lasers will be briefly discussed. The oldest laser is the ruby laser with ruby as the active medium. Ruby is the red variety of the mineral corundum, Al_2O_3 doped with 0.05 % Cr_2O_3, where the Cr^{3+} ion forms the active component. The laser, one of the very few three level-lasers, is pumped by flashing lamps and exists in both pulsed and continuous forms. The wavelength is 694.3 nm. In the experiment Nd:YAG lasers have been used as pump lasers. The active medium in this kind of laser consist of a crystal, Nd:YAG, $Y_3Al_5O_{12}$ with 1 % Y^{3+} replaced by Nd^{3+}. The laser, a four-level laser,is pumped either by a krypton lamp, the continuous variant, or by a xenon lamp, the pulsed variant. The wavelength is 1.06 μm.

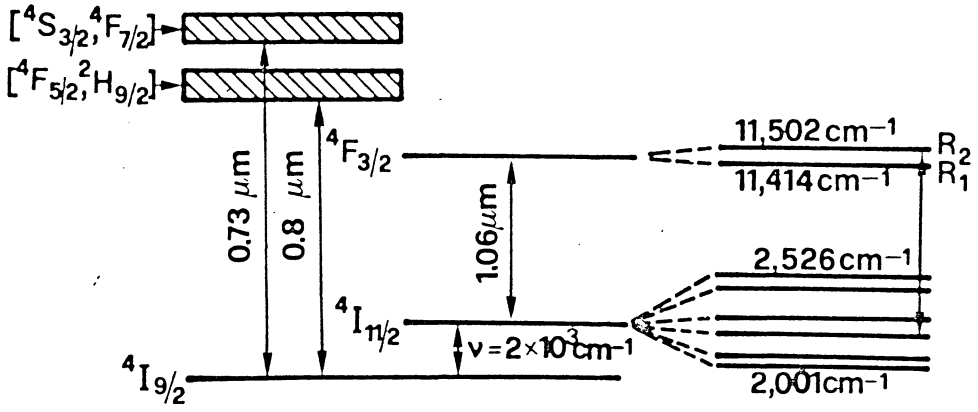

Fig. 1.5.2 Simplified energy levels of Nd:YAG [17].

The HeNe laser is a gas laser with the active medium consisting of a mixture of He and Ne gases. The He atoms are excited by electrical discharges, and the Ne atoms are then excited by collisions with the excited He atoms. The 2^1S and 2^3S levels of the He^* atoms are very close to the 3s and 2s levels of the Ne^* atoms and fore that reason energy is easily transferred between the atoms. The 2s and 3s levels of

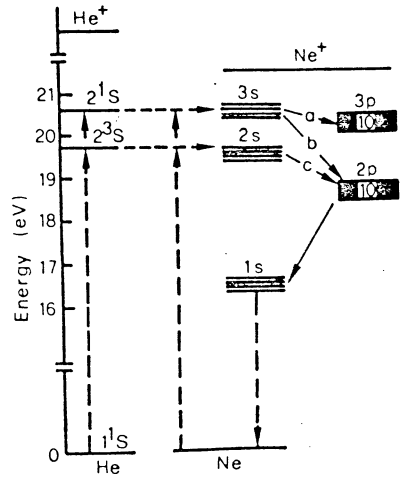

Fig 1.5.3 Energy levels of He and Ne [17].

the Ne^* atoms quickly decay to the 2p level. However, the transition 2p-1s is forbidden and during its life time an inverted population is created. After the stimulated emission of the 2p-1s transition the last level quickly decays to the ground level. The HeNe laser is thus a four-level laser.

The laser studied in this work is a dye laser, where the active medium is an organic dye dissolved in, for instance, methanol. The dye consists of large complex molecules with broadened rotational-vibrational bands. The laser transition occurs between the lowest-lying singlet bands in the ground state band where the molecules have a Bolzmann distribution. When pumped the molecules are excited to the upper S_1 band. The molecules are then de-excitated by relaxation to the lowest sub-level in the S_1 band. The transition to any of the sub-levels in the S_0 band is then mediated by stimulated emission. Due to relaxation in the upper band, the spectrum of the fluorescence light is independent of the spectral distribution of the pump light. The dye is contained in a cell which is placed in the cavity. A pump is used to circulate the fluid, as the pump light might deplete the dye. Both flash lamps and lasers can be used to pump a pulsed dye laser, but only lasers can be used to pump continuous lasers, as a focused laser beam is necessary to obtain the high power density needed.

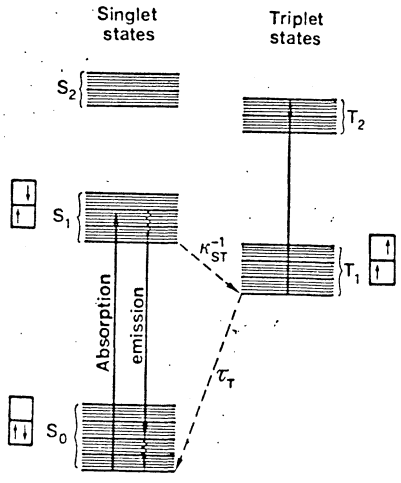

Fig 1.5.4 Typical energy levels for a dye in solution. The singlet and triplet levels are shown in separate columns [17].

2 Gratings and Fabry-Perot interferometers.

2.1 The diffraction grating.

In order to study the spectral distribution of light, one has to disperse it into its different components. The first decomposition of light observed by man was probably the rainbow, in which the dispersing elements are surging water drops. The first man-made instrument used to study the dispersion of light, the glass prism, is based on the same principle as water drops. The refractive indices of water and glass, as also other transparent dielectric materials, are dependent on the wavelength of light. The dispersive power, $\mathcal{R}$, of a prism is dependent on the dispersion of the material of the prism and is defined by;

$$\mathcal{R} = \frac{\lambda}{\delta\lambda} = b\,\frac{dn}{d\lambda} \qquad 2.1.1$$

where n is the index of refraction, $dn/d\lambda$ the dispersion and b the length of the base of the prism. Thus the dispersive power of all prisms is limited, as it is dependent on the material of which the prism is made.

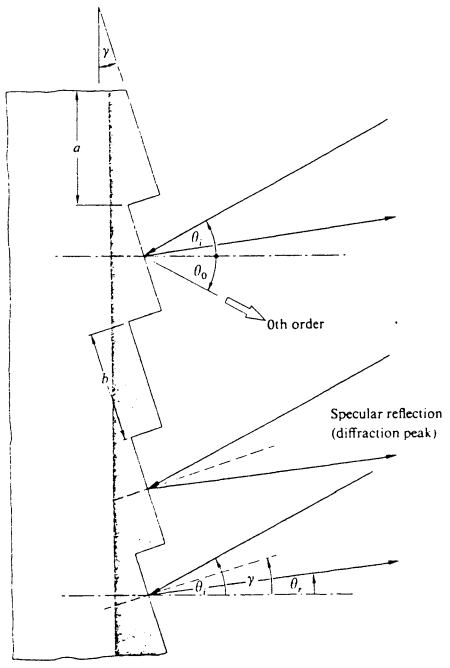

Fig 2.1.1 Section of a blazed reflection phase grating. Θ_i the angle of incidence, Θ_r the angle of reflection, γ; the blaze angle, a; the grating constant and b; the width of the grooves [18].

Gratings are a good solution since, based on a variation of the Fraunhofer diffraction principle, the diffraction is not dependent on the material used. The most common type is the reflective grating, where light is diffracted by grooves on its surface. An example of a reflective grating is shown above in fig 2.1.1. The the mutual distance between the N grooves is a, each with a width b. The angles of the incident, Θ, and refracted light, ϕ, are measured from the normal to the plane of the grating. In constructive interference the optical wavelength is an integral number of wavelengths and, as a consequence, we get the grating formula;

$$a(\sin\phi + \sin\Theta) = m\lambda \qquad 2.1.2$$

where m, an integer, denotes the order of the diffraction. The resolving power of a diffractive grating is

$$\mathcal{R} = Nm, \qquad 2.1.3$$

illustrating the necessity of illuminating the full grating. The angular dispersion, $\mathcal{D}$, is given by

$$\mathcal{D} = \frac{d\Theta}{d\lambda} \qquad 2.1.4$$

and by differentiating the grating formula;

$$\mathcal{D} = \frac{m}{a \cos\phi} . \qquad 2.1.5$$

The free spectral range of the grating, that is, the distance between two lines of identical wavelength but of adjacent orders, is given by

$$(\Delta\lambda)_{fsr} = \frac{\lambda}{m}. \qquad 2.1.6$$

Higher orders of diffraction will favour the resolving power and the angular dispersion but increases the risk of getting an overlap of adjacent orders of spectra.

The gratings are commonly produced as replicas from a master grating of glass with grooves made with a diamond tip. A novel way of producing

gratings is to register an interference pattern from a laser on a photo resist, placed on the surface of a glass plate. The grooves are then produced by etching. This method makes it possible to produce gratings with larger grating constant, a, than previously. To obtain gratings with better efficiency, the ruled grooves are given a controlled shape. With this kind of ruled grooves it is possible to produce gratings reflecting as much as 80 % of the incoming light into one particular order of a given wavelength. This kind of grating is called a blazed grating.

The echelle grating is specially designed to obtain high dispersion and spectral power by the use of high orders of interference. The ruled grooves of an echelle grating are, as in the case of the blazed grating, given a controlled shape, but the blaze angle is greater than 45^{o} and thus the angle of illumination must be greater than 45^{o}. The grating constant of this type of grating, however, is smaller than that of a more common type.

As a dispersive element in lasers, gratings have been used in a Littrow mount. The advantage of this type of arrangement is that the grating acts as a mirror, since the direction of the refracted light from the grating is opposite to that of the incident light, and thus replaces the fully reflecting mirrors in the laser cavity. Due to the Littrow condition $\phi = \Theta$, the grating formula becomes;

$$2a \cdot \sin\Theta = m\lambda. \qquad 2.1.7$$

For spectroscopic applications a combination of a grating and a plane mirror has been used in order to increase resolution and dispersion [1]. The principle of this arrangement is to let the mirror retro-reflect the diffracted light towards the grating. The orientation of the mirror determines the wavelength of the light that returns to the dye cell. For an arrangement of this type the angular dispersion

$$\frac{d\theta}{d\lambda} = \frac{2 \cdot m}{a \cdot \cos\theta} \qquad 2.1.8$$

is twice that of the Littrow case, as the light is defracted twice before returning to the dye cell. For the deduction of this formula see

Appendix A.2.

2.2 The plane Fabry-Perot interferometer.

The Fabry-Perot interferometer is one of the most commonly used interferometers in the sphere of laser spectroscopy, due to its extremely good dispersive power and simple design. The principle of the Fabry-Perot interferometer is based on multiple beam interference in connection with multiple reflection in a transparent plate of a dielectric material. The index of refraction of the plate differs from that of the dielectric material in which it is embedded. If coherent light consisting of parallel rays is incident on the plate, a part of the light will be reflected from the surface, and the other will be transmitted into the plate, where a large number of internally reflected rays will be produced. This effect will be enhanced if the amplitude-reflection coefficient, r, is large. Some of the light will be transmitted through the surfaces. Each ray has a defined phase different from the other reflected rays, due to differences in their the optical paths and to phase shifts occurring in the various reflexions. As the waves are coherent they will interfere if collected and focussed in a point. A plane wave is mathematically described by;

$$E(t) = E_0 e^{iwt} \qquad 2.2.1$$

where E_0 is the amplitude and ω the angular frequency of the light. Adding all the contributions from transmitted and reflected waves and considering the complex part of the plane wave, the Airy distribution is finally obtained;

$$I = \left[\frac{T}{1 - R}\right]^2 \frac{I_0}{1 + (1-R)^2 \sin^2 \frac{\phi}{2}} \qquad 2.2.2$$

T is here the transmittance, and R the reflectance. In fig 2.2.1 the Airy distribution is shown for some different values of r, where $r^2 = R$.

To increase the reflectance of the plate, its surfaces are covered with thin, partially transparent metallic films. The metal atoms will, however, absorb some light. The phase difference between two

successively transmitted waves, Φ, is

$$\Phi = \frac{2\pi\Delta}{\lambda} = \frac{4\pi}{\lambda} \, l \, n \cos \Theta_i. \qquad 2.2.3$$

$\Delta = 2nl \cos \Theta_i$ is the optical path difference, n the index of refraction of the glass plate and l the thickness of the plate. With a monochromatic light source and a Fabry-Perot interferometer with R $\approx$1, a system of concentric thin rings is obtained, the intensity distribution of which is described by the Airy distribution. The distance between two consecutive peaks of the Airy distribution or two consecutive rings is the free spectral range, $(\Delta\lambda)_{fsr}$, of the Fabry-Perot intereferometer and is expressed by;

$$(\Delta\lambda)_{fsr} \approx \frac{\lambda^2}{2nl}, \qquad 2.2.4$$

or,

$$(\Delta\nu)_{fsr} \approx \frac{c}{2nl} \, . \qquad 2.2.5$$

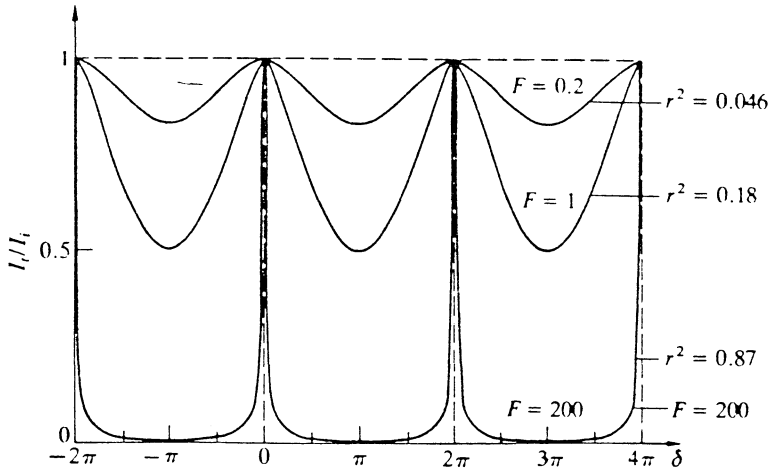

Fig 2.2.1 The Airy distribution [18].

The coefficient of finesse, F, is given by

$$F = \frac{4R}{(1 - R)^2} \qquad 2.2.6$$

The sharpness of the fringes is measured by the half width, γ, which is infered from;

$$\frac{1}{2} = [1 + F \sin^2(\frac{\gamma}{2})]^{-1} \qquad 2.2.7$$

Thus,

$$\gamma = 2 \sin^{-1} \frac{1}{\sqrt{F}} \approx \frac{2}{\sqrt{F}}, \qquad 2.2.8$$

if F is large and the resulting half width;

$$\gamma = \frac{4}{\sqrt{F}}. \qquad 2.2.9$$

The finesse, $\mathcal{F}$, is defined by the ratio between the free spectral range and the half width;

$$\mathcal{F} = \frac{2\pi}{\gamma} = \frac{\pi\sqrt{F}}{2} = \frac{\pi\sqrt{R}}{1-R} \qquad 2.2.10$$

Another parameter of importance, in terms of frequency, is the minimum resolvable band width, $(\Delta\nu)_{min}$;

$$(\Delta\nu)_{min} = \frac{c}{\mathcal{F}nd}. \qquad 2.2.11$$

based on the Rayleigh criterion for resolving two overlapping slit images of equal irradiance. The finesse may now be defined as

$$\mathcal{F} = \frac{(\Delta\nu)_{fsr}}{(\Delta\nu)_{min}}. \qquad 2.2.12$$

The resolving power is obtained by

$$\mathcal{R} = \nu \frac{2nl}{c} \mathcal{F}. \qquad 2.2.13$$

If the interference pattern or the ring system is pictured on a screen by a positive lens of focal distance f, the radii of the rings ρ_m are given by

$$\rho_m^2 = 2f (1 - \frac{m\lambda}{2nl}) \qquad 2.2.14$$

2.3 The confocal Fabry-Perot interferometer.

In this work a confocal Fabry-Perot interferometer was used as a spectroscopic device. In the following paragraphs the theory and the use of this type of interferometer will be discussed briefly.

The confocal Fabry-Perot interferometer differs from the ordinary one in that the pair of plane mirrors is replaced by a pair of spherical mirrors with a common radius of curvature and with a mutual distance equal to this radius. The advantages of the confocal Fabry-Perot interferometer over the plane one, that motivate its use, are a high light gathering power, freedom from mode-matching and the capability of the instrument to be used to display spectral information in the form of a multiple-beam, interference fringe pattern [12]. On the other hand, the instrument requires a very precise control of the distance between the mirrors, with the result that the free spectral range is fixed.

2.4 The Fringes.

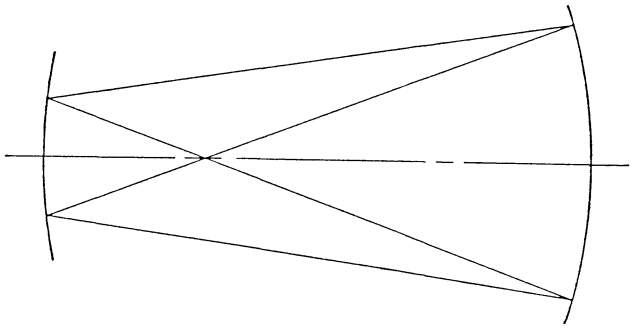

Fig 2.4.1 a) Ray path in a FPS in the paraxial approximation (reentrant rays) [12].

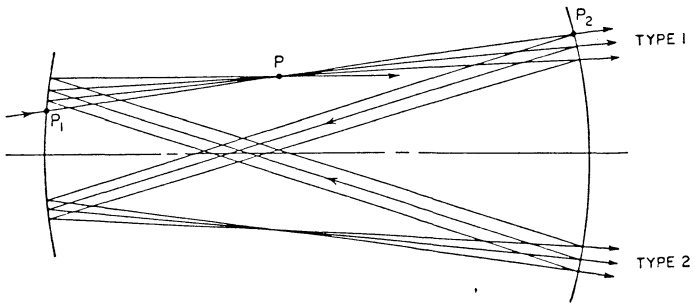

b) Abberated ray path, showing intersection of rays at point P [12].

The focal distance of a spherical mirror, f, with a radius of curvature, r, can be stated as

$$f = \frac{r}{2} \qquad 2.4.1$$

This implies that a paraxial ray makes 2 double passes in a confocal resonator. For an ideal resonator the ray will, after traversing the resonator 4 times, be re-entrant i.e, fall back onto itself, as shown in fig 2.4.1a above. In a real resonator, however, a general ray is not re-entrant due to aberrations in the mirrors. The ray will, however, continue to intersect itself at the vicinity of a point P, located in the central plane of the interferometer, at a distance ρ, from the axis, (see fig 2.4.1b). The shape of the fringe pattern is determined by the positions of the points at which the rays intersect. Assuming a small and distant light source, placed close to the axis, the path difference $\Delta\rho$ between the four transition paths and the paraxial path $4(r+\varepsilon)$ is

$$\Delta(\rho) \cong \rho^4/r^3 + 4\,\varepsilon\,\rho^2/r^2 \qquad 2.4.2$$

where the mirror spacing is $(r + \varepsilon)$. Two sets of transmitted rays are generated by each incident ray, those which have been reflected 4 m times and those which have been reflected (4 m + 2) times where m is an integer, (see fig 2.4.2 below).

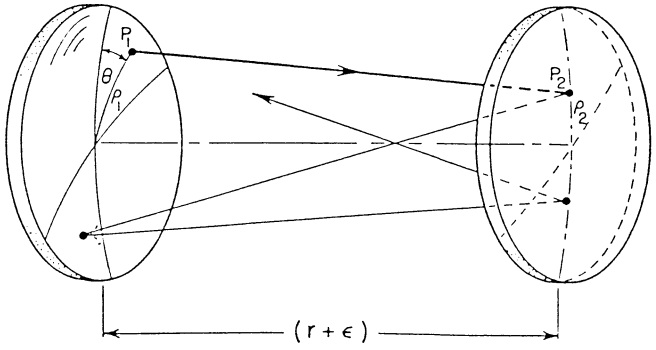

Fig 2.4.2 General ray path in a spherical mirror Fabry-Perot interferometer [12].

The interference pattern produced in the central plane of the interferometer is given by;

$$I_1(\rho,\lambda) = I_o\left[\frac{T}{1-R^2}\right]^2 \frac{1}{1+\left[\frac{2R}{1-R^2}\right]^2 \sin^2 \frac{\delta(\rho,\lambda)}{2}} \qquad 2.4.3$$

for rays of the first type and for the second type:

$$I_2(\rho_1\lambda) = R^2 I_1(\rho,\lambda), \qquad 2.4.4$$

where

$$\delta(\rho,\lambda) = \frac{2\pi}{\lambda}[\Delta(\rho) + 4(r + \varepsilon)] \qquad 2.4.5$$

For values of the mirror reflectivity, R, close to unity, two types of rays will be the same and superposed. An interference pattern with equally spaced and straight fringes will be produced if the beam is collimated and at an angle to the axis, and if the two beams are coherent. The bright circular fringes are formed when

$$\delta(\rho,\lambda) = 2m\pi \qquad 2.4.6$$

or

$$\rho^4/r + 4\varepsilon\rho^2/r^2 = m\lambda \qquad 2.4.7$$

where m is a positive or negative integer representing the order of interference relative to the order on axis. The corresponding fringe radius is given by

$$\rho_m = \sqrt{-2\varepsilon r\lambda \sqrt{4(\varepsilon r)^2 + m\lambda r^3}} \qquad 2.4.8$$

2.5 Spectral Resolving Power

One of the most important properties of the Fabry-Perot interferometer is its spectral resolving power $\mathcal{R}$;

$$\mathcal{R} = \frac{\nu}{\Delta\nu_m} \qquad 2.5.1$$

$\Delta\nu_m$ is the minimum resolvable increment of the frequency in the vicinity of a frequency ν. Usually the minimum resolvable band width is defined as the full width at half maximum of the instrumental function. The latter is the spectral profile which would be observed with a purely monochromatic source . The resulting value for $\Delta\nu_m$ is;

$$\Delta\nu_m = c(1-R^2)/\ 4\pi r\mathcal{R}. \qquad 2.5.2$$

An important quality of a Fabry-Perot interferometer is the finesse, $\mathcal{F}$, defined as the ratio of free spectral range to instrumental width

$$\mathcal{F} = \frac{\Delta\nu_{fsr}}{\Delta\nu_{min}} \qquad 2.5.3$$

As $\Delta\nu_{fsr} = \frac{c}{4r}$, the instrumental width is $\Delta\nu_m = \frac{c}{4r\mathcal{F}}$

and the resolving power

$$\mathcal{R} = \frac{c}{\lambda} \cdot \frac{1}{\Delta\nu_m} = \frac{4r\mathcal{F}}{\lambda}. \qquad 2.5.4$$

The reflectivity finesse is given by

$$F_R = \frac{\pi R}{(1-R^2)} \approx \frac{\pi}{1-R}\ , \qquad 2.5.5$$

for $R \approx 1$.

The most important factors when determining the finesse of the confocal Fabry-Perot interferometer is the reflectivity of the mirrors and irregularities on surfaces. If no other losses occur the finesse is limited by the reflectivity finesse. If the mirrors have a smooth irregularity of the order of $\frac{\lambda}{m}$ the resulting finesse F_α limited by the figure of the mirrors will approximately be;

$$F_\alpha = \frac{m}{2}. \qquad 2.5.6$$

However, for a confocal Fabry-Perot interferometer it is possible to minimize the reduction of the instrumental finesse due to plate regularities by reducing the aperture. An angular misalignment of a mirror will not affect the instrumental finesse, as the only effect will be a redefining of the optical axis. The losses due to diffraction are

very small compared to the plane mirror Fabry-Perot interferometer. Diffraction losses are minimized if the interferometer is mode-matched.

The net instrumental finesse F is related to the individual contributions F_i by

$$F^{-1} = \Sigma\ (F_i)^{-1} \qquad 2.5.7$$

To each loss mechanism, a contribution to the cavity life time can be associated. To the i:th loss mechanism, the associated finesse F_i is related to the corresponding cavity life time τ_i by

$$F_i = \frac{\pi c \tau_i}{2r} \qquad 2.5.8$$

To obtain the ultimate instrument profile for the scanning mode of operation the detector aperture must be vanishingly small. With a finite aperture the instrument profile is not symmetric and not centred on ν_0, which is the frequency recorded by using the smallest aperture possible.

2.6 Light Gathering Power

When using the spectrometer the aperture with an area A is illuminated by some kind of light source. All the light from the light source that falls onto the aperture, emanates within a solid angle Ω and is transmitted within the band pass $\Delta\nu_n$ of the spectrometer. The radiant power per unit band width P_ν transmitted by the spectrometer is

$$P_\nu = N_\nu\ A\ \Omega\ T_o \qquad 2.6.1$$

where T_o is the transmission of the spectrometer at the centre of the band pass and N_ν the radiant power per unit band width. Defining the etendue of the spectrometer

$$U = A\ \Omega \qquad 2.6.2$$

we obtain

$$P_\nu = N_\nu\ UT_o \qquad 2.6.3$$

When studying laser light the etendue of the spectrometer provides a measure of the alignment tolerance between the laser beam and the spectrometer. The transmission T_o at the centre of the instrument profile may be written;

$$T_o - (1+R^2)\frac{T}{1-R^2} \approx \frac{1}{2}\left[\frac{T}{1-R}\right]^2 \qquad 2.6.4$$

for $R \approx 1$. This expression is obtained from the expressions of the two transmitted beams evaluated from a single beam of light incident on a confocal Fabry-Perot interferometer. If the sum of absorption and scattering in the mirrors is A then $1-R = T+A$, resulting in

$$T_o \approx \frac{1}{2(1+A/T)^2}. \qquad 2.6.5$$

A high finesse is achieved at the expense of the transmission. As stated earlier the ultimate instrumental resolution R_o, is obtained with a point-like axial aperture. Consequently the etendue will also be infinitesimal. However, a reasonable resolution is obtained with an aperture that gives a resolving power of about 0.7 R_o. The corresponding etendue is thus given by

$$U = \pi \nu^2 \lambda/F. \qquad 2.6.6$$

A useful compromise between resolution and transmitted power is quickly obtained by starting with a large aperture and reducing it until the transmitted power of the displayed spectral line is reduced by about 25 %. The interferometer should be operated in the scanning mode and the light source used should be of the narrow band type.

The eigenmode structure of a resonant cavity is denoted TEM_{mnq}, where m and n denote the amplitude distribution on a surface of constant phase and q denotes the axial mode number. For a confocal or near confocal resonator the resonant frequency is given by

$$\nu_{mnq} \approx [c/4(r+\varepsilon)]\ [2q + (1 + m + n)]. \qquad 2.6.7$$

The resonant length of a given combination of m, n and q is given by

$$(r + \varepsilon) \approx \frac{c}{4\nu_o} [2q + (1 + m \cdot n)] \qquad 2.6.8$$

where ν_o is arbitrary, quasi-monochromatic light incident on the resonator. If light of frequency ν_o is made up of an approximately equal number of even and odd modes the cavity will be resonant for

$$(r + \varepsilon) - \frac{cl}{4\nu_o} ; \qquad 2.6.9$$

where l is an integer and the corresponding free spectral range

$$\Delta\nu_{fsr} = c/4r; \qquad \text{multi mode.} \qquad 2.6.10$$

But if the input light exactly matches a single mode of the cavity then

$$\Delta\nu_{fsr} = c/2r; \qquad \text{single mode.} \qquad 2.6.11$$

As a consequence of mode-matching, the two types of transmitted rays are aligned, and are in phase on axis, just out of phase at the first fringe off axis, in phase for the second fringe off axis and so on. Also the transmitted light is doubled at a given resonance. It is not necessary, however, to mode-match the interferometer to obtain a clean spectrum. The tolerance in the alignment of the light beam relative to the optical axis is very small and mode-matching is not encountered inadvertently.

2.7 The design of the confocal Fabry-Perot interferometer.

The design of a confocal Fabry-Perot interferometer consists of a fixed mirror cell, a thermally compensated rigid spacer tube, including a piezo-electric ceramic section, and an adjustable mirror cell. The Fabry-Perot etalon is contained in the outer case and mechanically isolated from this. In the outer case, mountings are provided for an adjustable lens in the front and a photo detector at the other end. The construction of the interferometer is shown in fig 2.7.1 below.

When used in the scanning mode the interferometer should be mounted in so that the entire instrument is rotated about the entrance aperture.

This is desirable as it makes the alignment easier. It is also desirable to design the mounting of the instrument in such a way that it can be moved with its axis parallel to the beam in two mutually perpendicular directions, see fig 2.7.2 further below .

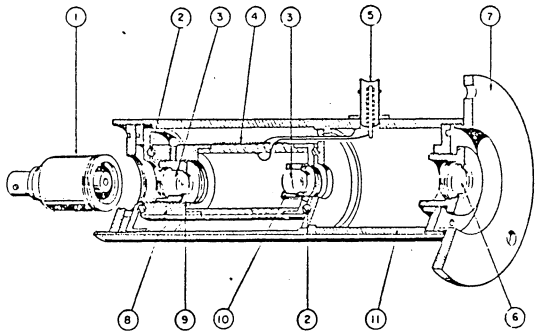

Fig 2.7.1 A FPS spectrum analyzer for scanning or static mode of operation. 1) removable detector (photo diode); 2) soft O-ring for mounting FPS etalon; 3) quartz mirrors (r = 5 c m); 4) piezo-electric transducer/etalon spacer; 5) scanning voltage terminal; 6) auxiliary lens (focal point is between mirrors); 7) mounting flange; 8), 9) adjustable mirror cell; 10) fixed mirror cell; 11) outer case [12].

To align the instrument in the scanning mode the photo detector is demounted and held in the beam by a pinch. Then the instrument is placed in the beam with its axis roughly aligned with the beam. The final adjustment is made by the aid of the reflected light from the instrument, which should be adjusted to lie fairly close to the incident beam. If properly aligned transmitted light will reach the photo detector. To make a fine adjustment a saw-tooth voltage is applied to the scanning voltage terminal. The output of the instrument is monitored by an oscilloscope connected to the photo diode. The alignment of the instrument and if necessary the distance between the mirrors is adjusted until the desired light and shape of the peaks are obtained. Then the photo detector is mounted on the instrument again.

If the instrument is used to observe interference fringes, the lens and photo detector are removed and the incident beam is directed towards the end of the instrument at which the detector was located. The fringe pattern can be viewed directly through the lens or through a telescope,

(compare with fig 2.7.2c below). It can also be reproduced on a screen. The angular alignment of the instrument is made until a sharply defined and circular symmetric fringe pattern is obtained. To make a fine adjustment, the mirror separator is brought closer together by a fraction of a wavelength. At the same time the range of the control fringe must be observed. If the diameter of the central fringe becomes smaller the mirror separation is greater than the confocal separation. If on the other hand the central fringe diameter becomes greater the corresponding mirror separation is smaller than the confocal separation.

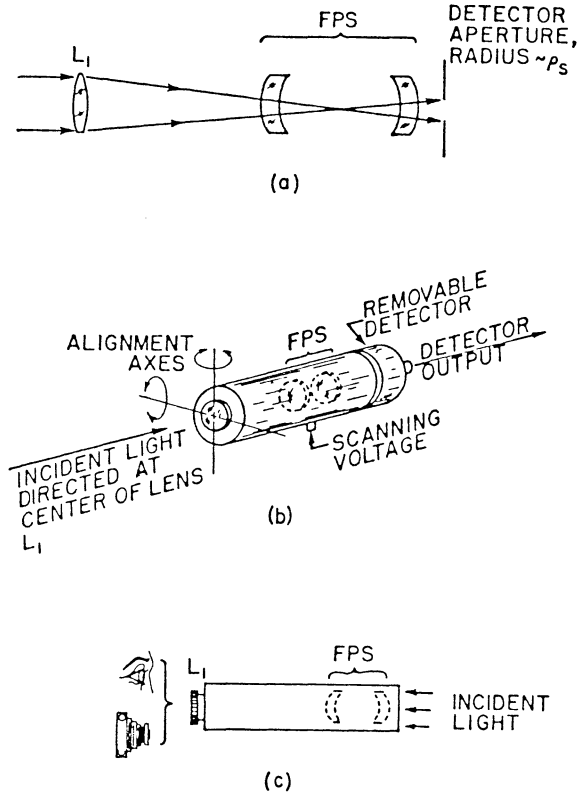

Fig 2.7.2 A versatile FPS instrument. a) Optical layout showing the FPS etalon, lens L_i and detector aperture; b) arrangement for scanning; c) arrangement for observing and recording fringe patterns (detector removed) [12].

3 The Hänsch laser.

3.1 Introduction.

In the beginning of the 1970's T W Hänsch presented a novel laser design [5]. At that time the purpose of the pulsed laser design was to achieve lasers that offered narrow bandwidths, convenient, reproducible wavelength tuning and good stability.

The usual way to obtain a tunable, narrow band laser was to put some kind of dispersive element in the cavity, such as a lense, a prism or a grating. Using long-pulse, flashlamp-pumped, dye lasers narrow band linewidths are easily achieved even with wavelength selectors of low dispersion. With prisms or lenses as dispersive elements, a bandwidth of a fraction of 1 Å was obtained. On the other hand, for dye lasers side-pumped by a short-pulsed laser such as a nitrogen laser, linewidths below 10 Å seemed to be very difficult to achieve, even with high a dispersive grating, due to the limited number of light passes and the small diameter of the pump beam. However, a nitrogen-pumped, dye laser with a short cavity length in conjunction with a combination of a holographic grating and a Lyot-filter was operated in the single mode with a bandwidth of about 0.01 Å, but the reproducibility from shot to shot was poor.

3.2 The Hänsch design.

In his design Hänsch replaced the 100 % mirror with a high order echelle grating in a Littrow mount [5], (see fig 3.2.1). The grating will perform as a mirror when the equation for the Littrow arrangement,

$$2a \sin \theta = m\lambda, \qquad 3.2.1$$

is satisfied, and thus one mirror in the cavity is omitted. In this equation the angle of incidence is θ, a is the groove spacing, m an integer and λ is the wavelength. Tuning is achieved by mechanically turning the grating around an axis parallel to the grooves. The tuning range is limited by the separation of adjacent grating orders and the angle dispersion is given by

$$\frac{d\theta}{d\lambda} = \frac{m}{a \cdot \cos\theta} = \frac{2 \cdot \tan\theta}{\lambda} \qquad 3.2.2$$

At the other end of the optical cavity a planar out-coupling mirror is mounted.

Due to the high losses in very narrow-band, wavelength selectors, such as gratings, a high gain of the dye will be necessary to make the laser operate. This condition will be met, however, since an unsaturated single pass gain of 30 dB of a path length of a few millimeters is easily achieved with a dye medium pumped with a nitrogen laser [2].

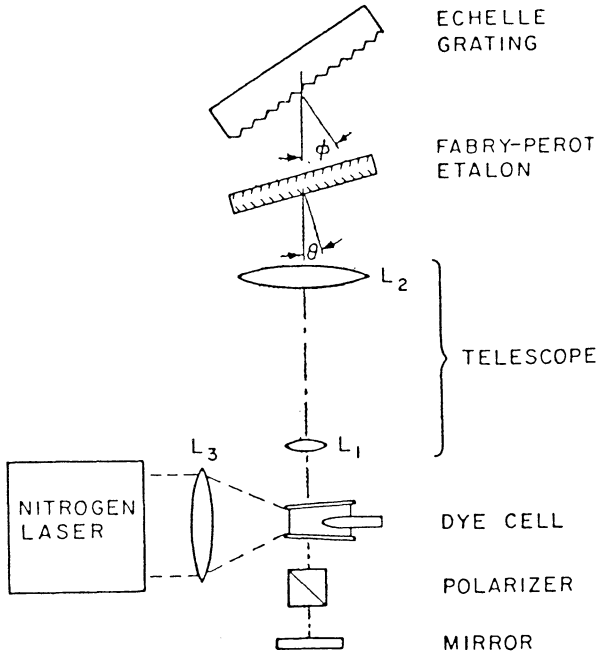

Fig 3.2.1 Basic components of narrow-band, tunable dye laser [5].

In the dye cell only a small volume near the inner wall is excited by the pump light. As a result diffraction will cause a considerable angular spread of the emerging light, and will consequently reduce the resolution of the grating.

An inverted telescope placed in front of the grating will collimate the beam and with properly selected lenses spread the beam over the entire grating, thus enhancing the resolution of the grating. The use of a telescope will also prevent the surface of the grating from being destroyed by light intensities which are too high.

In his design Hänsch used a Fabry-Perot etalon in order to further reduce the linewidth. Fine tuning is achieved by mechanically rotating the etalon along an axis parallel to the grooves of the grating. Between the dye cell and the out coupling mirror an optional Glan Thompson polarizer is placed to increase the efficiency of the laser by polarizing the light orthogonally to the grooves. The laser is tunable through several Å if the grating and the etalon are rotated simultaneously.

4 The first grazing-incidence, pulsed, dye lasers.

4.1 Why develop the Hänsch design?

The Hänsch laser design was a major advance in the development of pulsed dye lasers, but the method of expanding the beam made the laser difficult to operate. Other ways of expanding the intra-cavity beam were the use of a prism, multiple prisms or a mirror telescope, but these did not make the laser easier to use. The problems with the intra-cavity expansion were difficult alignment procedures and the need for frequent focusing adjustments. The cavity became too long, resulting in only a few cavity round trips. The introduction of optical components resulted in a poor beam quality. There was no need for two-dimensional expansion. Another drawback was the necessity of using an extremely precise rotational mechanism to keep the grooves of the grating orthogonal to the laser axis as the grating is rotated. Efforts were made to find a design without any cumbersome beam expansion. The solutions presented here were presented by Shosan et al. [6] and independently by Littman et al. [7], [8].

Due to the small number of round trips in the cavity, the bandwidth of the laser may be represented by the single pass bandwidth given by;

$$\delta\lambda = \frac{2 \cdot \delta\alpha}{d\theta/d\lambda}, \qquad 4.1.1$$

where $\delta\alpha$ is the half angle divergence of the intra-cavity beam. The usual way of reducing the bandwidth $\delta\lambda$ is to reduce the divergence, $d\Theta/d\lambda$, by collimating the beam inside the cavity and to use a highly dispersive grating at high angle of incidence.

4.2 Grating at grazing incidence.

Another way of reducing the bandwidth is to increase the denominator of the equation (4.1.1) by increasing the angle of incidence onto the grating. However, at angels of incidence much higher than 75^{o} the efficiency of the grating is very low. To make the laser work in an efficient way, the output-coupling mirror must be replaced by a fully reflecting mirror [6], [9]. The beam is coupled out from the grating by the

zero order of refraction. By making the cavity as short as possible, several cavity round trips are possible during the short lasing time. In this way the faint back diffracted light from the grating will be sufficient to build up and maintain an inverted population in the dye during the short pump time. The Shosan solution is shown in fig 4.2.1 below.

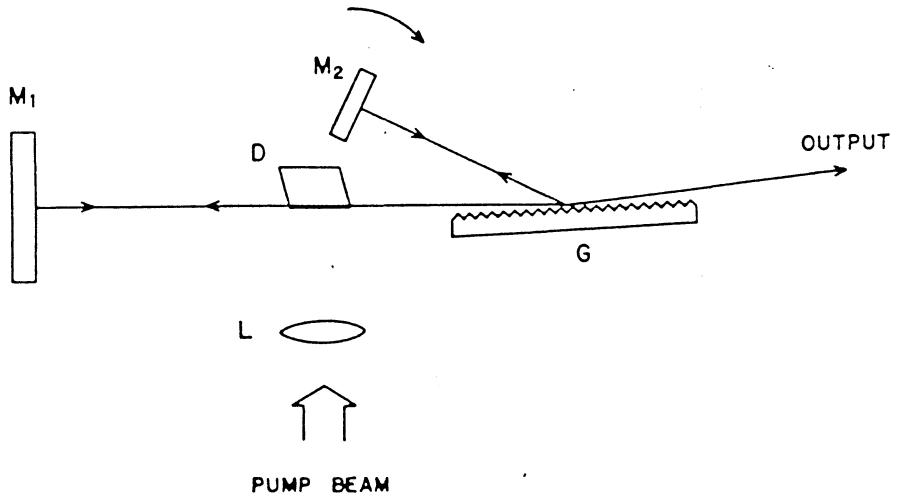

Fig. 4.2.1 The dye laser cavity: M_1, fixed 100% mirror; M_2, rotatable mirror; D, dye cell; L, cylindrical lens; G, diffraction grating [6].

Unfortunately the Littrow mount has some disadvantages. A serious problem is that almost no grating, developed for such a high angle of incidence, is available commercially making it necessery to produce a special one suitable for the high incidence angle used here. Another problem is that not only the wavelength but also the linewidth is highly dependent on the angle of rotation when tuning and thus the bandwidth of the light is changed with θ.

By replacing the Littrow mount by a combination of grating and mirror shown in fig 4.2.1 above, the disadvantages of the Littrow mount can be avoided and at the same time the dispersion will be doubled. With the expression for angular dispersion given in eq. 2.1.8 an expression for the bandwidth is obtained from

$$\delta\lambda = \frac{2\,\delta\alpha}{d\theta/d\lambda} = \frac{a\cos\Theta}{m}\,\delta\alpha \qquad 4.2.1$$

It is obvious that the bandwidth decreases when $\frac{a}{m}$ is made smaller and when θ is as large as possible, i. e. the grating is working at grazing incidence. By working with a higher order of the diffracted light it is possible to get light that is mixed with light of somewhat different wavelength. The mixing light originates from adjacent orders to both sides of the working order. The corresponding spectrum will contain many narrow peaks. A way to eliminate this disadvantage is to use a small mirror placed far away from the grating. Another simple way to solve this problem is to use the light from the first order, which gives a pure spectrum but with larger linewidth. By choosing a grating, meeting the requirement, $0.5\lambda < a < \lambda$, where λ is the wavelength used, one will get a spectrum containing only light of the first order.

With a grating working with many orders of diffraction it is necessary to tilt the grating in order to prevent unwanted feed-back to the dye cell. This kind of feed-back occurs when the condition of the Littrow reflection is satisfied. If the out-coupling mirror is replaced by a 100 % mirror, the zero order of reflection of the grating is used as out coupling, which gives enhanced conversion efficiency. But, on the other hand, the ASE (Amplified Spontaneous Emission) in the laser will increase. The linewidth can be decreased if a Fabry-Perot etalon is placed in the cavity. The arrangement will thus work as a narrow bandwidth filter, but, the use of the etalon will decrease the output power. The grating must be chosen with great care. The grating will be used twice on each cavity round trip, as the incident light is refracted towards the mirror and then reflected by the mirror towards the grating and again refracted, which gives the total efficiency as the square of the efficiency of the grating. It should also be observed that the efficiency of a holographic grating is greatest for light polarized at right angles to the grooves. Finally, decreasing the concentration of the dye to about $6 \cdot 10^{-4}$ M and shortening the cavity will make the laser work in the single mode at the expense of the output efficiency and the stability of the laser intensity.

This design of pulsed dye laser is comparable to the Hänsch design, concerning to the linewidth, lasing efficiency, tuning range and beam divergence. The advantages of using a grating at grazing incidence are great as the expensive beam expander is eliminated, alignments are easier

and losses due to reflections are small, as the cavity contains fewer optical components and consequently fewer surfaces. With the reduction of the number of components the sensitivity of the laser to temperature changes is decreased and the laser is not so vulnerable to high power beams. Finally, the grating can be made of a thin strip and the cavity length can be made more compact, thus using the short-duration pump light more efficiently.

5 Some developments of the pulsed grazing incidence dye laser.

5.1 Laser cavity with two gratings.

The beam expander in the Hänsch design described in previous chapters is a telescope, a prism or a combination of prisms. But as two-dimensional expansions of the beam was non crucial for the performance of the laser, it was desirable to develop a beam expander device working only in one dimension.

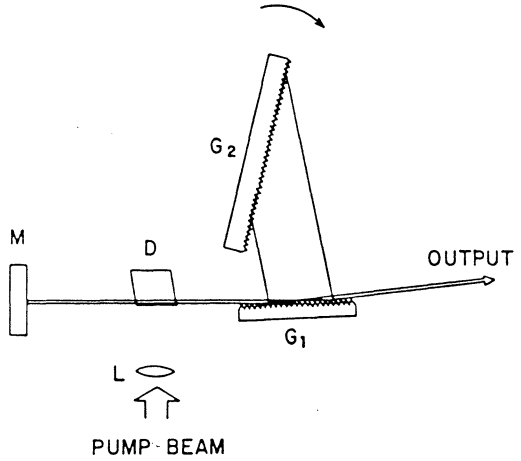

Fig 5.1.1 The dye laser cavity; M - 100% mirror; D - dye cell; L - cylindrical lens; G_1- grating expander; G_2- echelle grating in the Littrow mount [9].

In 1978 I Shoshan and U P Oppenheim [9] presented a design , see fig 5.1.1, with a grating at grazing incidence which thus also acted as a beam expander, fig 5.1.2. As a tuning device, a grating in the Littrow mounting was used. To understand the principles of this beam expander one has to return to the grating formula;

$$\sin \Theta + \sin \phi = \frac{m\lambda}{a}, \qquad 5.1.1$$

where a is the groove spacing, Θ is the angle of the incident beam, ϕ the angle of the refracted beam and m the order of diffraction. A magnification factor M defined as the ratio of the widths of the diffracted beam and the incident beam is expressed by

$$M = \frac{\cos \phi}{\cos \Theta} \quad . \qquad 5.1.2$$

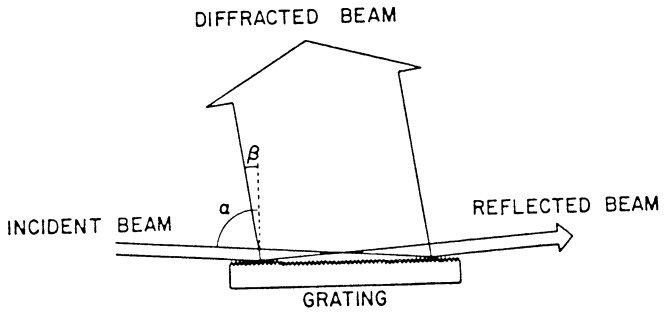

Fig 5.1.2 The beam expanding grating [9], α corresponds to Θ and β to ϕ.

To obtain a large M, a small ϕ and a large Θ are required. For a properly selected groove spacing, a small ϕ is obtained at grazing incidence. M also depends strongly on the angle of incidence Θ . Another benefit of this type of beam expander is that it diminishes the beam divergence. An incident monochromatic beam with a divergence $\delta\Theta$ is diffracted with a smaller divergence $\delta\phi$ given by

$$\delta\phi = - \frac{\cos \Theta}{\cos \phi} \delta\Theta = - M \delta\Theta. \qquad 5.1.3$$

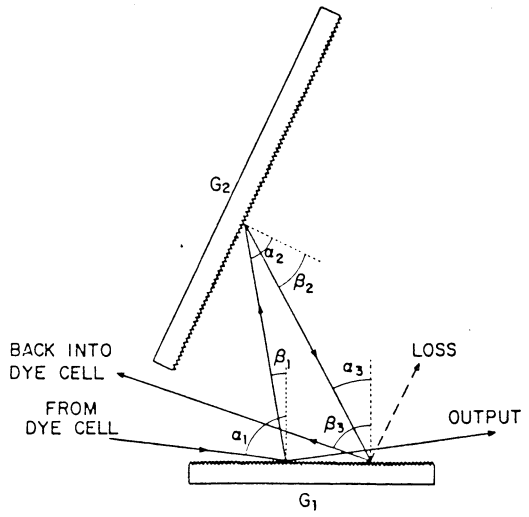

Fig 5.1.3 Ray diagram for the two gratings [9], Θ_j corresponds to α_j; $j \in \{1,2,3\}$ and ϕ_k to β_k, $k \in \{1,2\}$.

This equation is obtained by differentiating the grating equation 5.1.1. The total angular dispersion of this laser design is given by

$$\frac{d\Theta_3}{d\lambda} = M\left[\frac{2m_1}{a_1 \cos \phi_1} + \frac{m_2}{a_2 \cos \phi_2}\right] \qquad 5.1.4$$

with a_1, a_2 the groove spacings of the two gratings, and m_1, m_2 the corresponding diffraction order, (see fig 5.1.3). This equation is based on the fact that the intra-cavity beam is diffracted three times, twice in the beam-expanding grating and once in the tuning grating. The single pass band-width is given by

$$\delta\nu = \frac{2\,\delta\theta}{M\lambda^2\left[\frac{2m_1}{a_1 \cos \phi_1} + \frac{m_2}{a_2 \cos \phi_2}\right]} \qquad 5.1.5$$

where $\delta\theta$ is the half-angle divergence of the beam emerging from the dye cell. The single pass band-width is a relevant measure of the band-width of the cavity as there are very few round trips in the cavity. The gratings are mounted in the cavity with the direction of the grooves mutually parallel and with both planes of incidence coinciding. If the gratings are oriented as shown in Fig 5.1.3 the beam expanding grating contributes an additional dispersion to that obtained by the tuning grating.

5.2 Grating at grazing incidence combined with a Fabry-Perot etalon.

A Fabry-Perot etalon was placed in the laser cavity and the effect of this measure on the line width and the possibility of attaining a reliable single-mode operation were studied. Two ways of using a Fabry-Perot cavity are discussed, in the first the rear reflector is replaced by a resonant reflector, and in the second a Fabry-Perot etalon was placed in front of a fully reflecting rear mirror. The former study was performed by S Saikan [11] and the latter by T Chang and F Y Li [10].

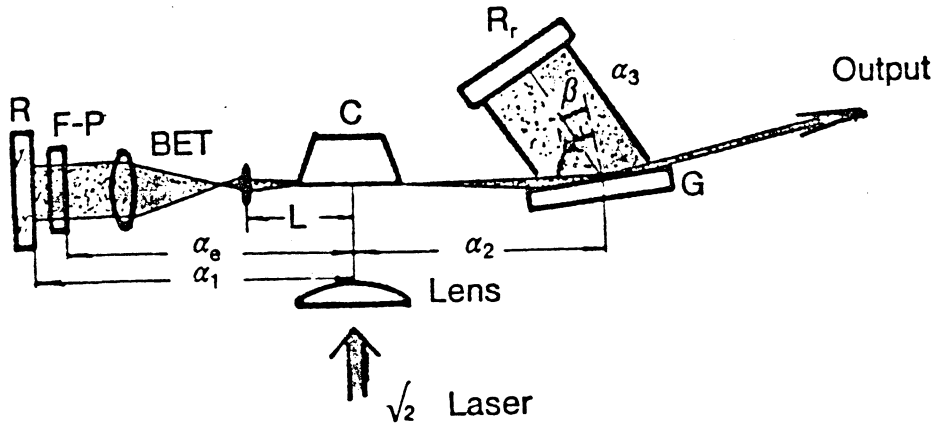

Fig 5.2.1 Schematic view of the optical arrangement of a pulsed dye laser with grating and etalon in a symmetric arrangement: R, reflecting mirror; F-P, etalon; C, dye cell; G, grating; BET, beam expanding telescope; R, tunable mirror [10].

In a laser cavity several modes can be found oscillating simultaneously. A single mode is selected by placing a Fabry-Perot etalon in the laser cavity. The mode of the laser cavity near the transmission maximum of the Fabry-Perot cavity will suffer the smallest losses of transmission and will thus oscillate alone while the others are suppressed.

Chang and Li [10] used a low-finesse, Fabry-Perot etalon together with a beam expanding telescope (BET) with low amplification. With a proper choice of the lenses and focal distances for the BET and the distance from the BET to the dye cell, they were able to reduce the band-width obtained by the etalon alone. Their design is shown in fig 5.2.1.

A resonant reflector is basically a reflecting Fabry-Perot etalon, and by using this instead of a mirror, Saikan [11] was able to reduce the cavity length and thus allow the laser to be pumped more effectively by the short-pulse-duration pump-laser. Since a shorter cavity allows more cavity round trips than a longer one during the short pump-laser time the intra-cavity light will interact with the same portion of the dye and thus encourage mode competition. Under these conditions a single axial-mode is readily attained. As a resonant reflector either two uncoated glass wedges, each at a distance of 3 cm were used or one or two quartz

glass plates, each 2.34 cm thick. To obtain a well defined mode structure and to keep clear of the lasing threshold a rear reflector was used, but when using a highly reflecting mirror the amplified, spontaneous emission dominates the output spectrum.

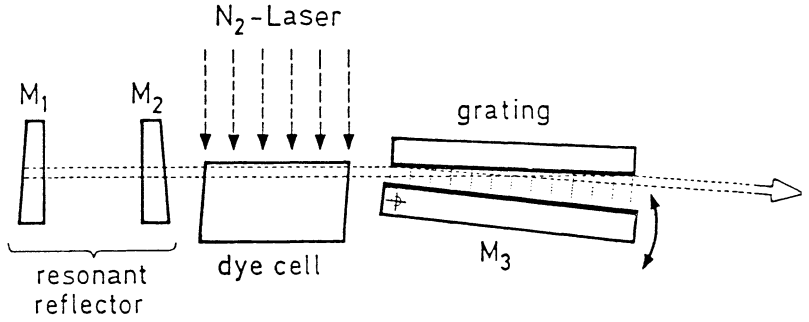

Fig 5.2.2 The dye laser cavity [11].

The dye cuvette was side-pumped by a nitrogen laser operated at a repetition rate of 30 Hz and with a pulse width of 3 ns (FWHM). Excitation powers of up to 50 kW were used. The dye consisted of courmarine 153 in ethanol. First the resonant reflector was replaced by a 100 % reflecting dielectric mirror, in order to observe multi-mode emission. The light was analyzed by a Fabry-Perot interferometer with a free spectral range of 0.5 cm^{-1}. Four axial modes were observed with a mode-spacing of 0.05 cm^{-1}. The corresponding effective cavity length was 10 cm, which corresponds to the length measured to the middle of the grating. The mirror was replaced by one or two resonant reflectors whose free spectral range was 0.14 cm^{-1} or 0.7 cm^{-1}. The spectrum was analyzed by a Fabry-Perot etalon with a spacing of 4 cm. The result, after averaging many measurements, was a line width of 420 ± 30 MHz for the single-mode output. This is very near to the Fourier transform limit. When the fully-reflecting mirror was used as end reflector, single-mode lasing was obtained only in the vicinity of the lasing threshold and the number of axial modes was dependent on the excitation power. When the mirror was replaced by the resonant reflector, single-mode oscillation was obtained for considerably higher excitation powers. A more stable single mode oscillation was obtained with two plane reflectors, since the value of the free spectral range was reduced to half of the original, resulting in an increased axial-mode selectivity.

6. The Littman concept

6.1 Introduction

With a grating used at grazing incidence a pulsed dye laser with a small line width and tunability over a large range was obtained.

The aim for further development was now to obtain a laser that was tunable in single mode. A solution of this problem was presented by M. G. Littman 1984 [12]. To make the laser work in single mode the cavity length was shortened to allow the intra-cavity light to make about 10 passes during the pump time. Another essential step was to define an optical path through the dye cell by focusing the pump light to an extremely small spot and by longitudinal pumping. In this way the same position in the dye will be used at each cavity pass. As the intra-cavity light makes about 10 passes through the homogeneously broadened medium there will be a natural tendency for the laser to run in single mode. This is further enhanced by the fact that the light, passing the dye through a very narrow cannel on each cavity round trip, will interact with the same portion of the dye, thus encouraging mode competition [12].

6.2 The Geometry of the Littman laser.

In previous designs, tuning was possible but mode jumps occurred. In a paper Littman and Liu [13] demonstrated that the combination of mirrors and grating possessed a specific point, which, when used as the pivot of rotating the tuning mirror, made tuning without mode-jumps possible. Rotating the tuning mirror about the pivot point to the tracking condition, i. e. simultaneously scanning the cavity length and the grating feedback angle, is satisfied exactly over the entire tuning range of the grating. But what conditions must be satisfied to obtain tracking?

1 The grating equation must be satisfied:

$$m\lambda = a(\sin \Theta_0 + \sin \phi) \qquad 6.2.1$$

where m is the diffraction order and a the distance between the grooves, Θ_0 the angle of incidence and ϕ the angle of diffraction.

2 The resonance condition;

$$N\lambda/2 = L(\phi) \qquad 6.2.2$$

of the cavity must be fulfilled, here N is the number of modes and $L(\phi)$ the length of the cavity, dependent on ϕ.

3 The angle of incidence must be very close to 90^{o}, for all ϕ's.

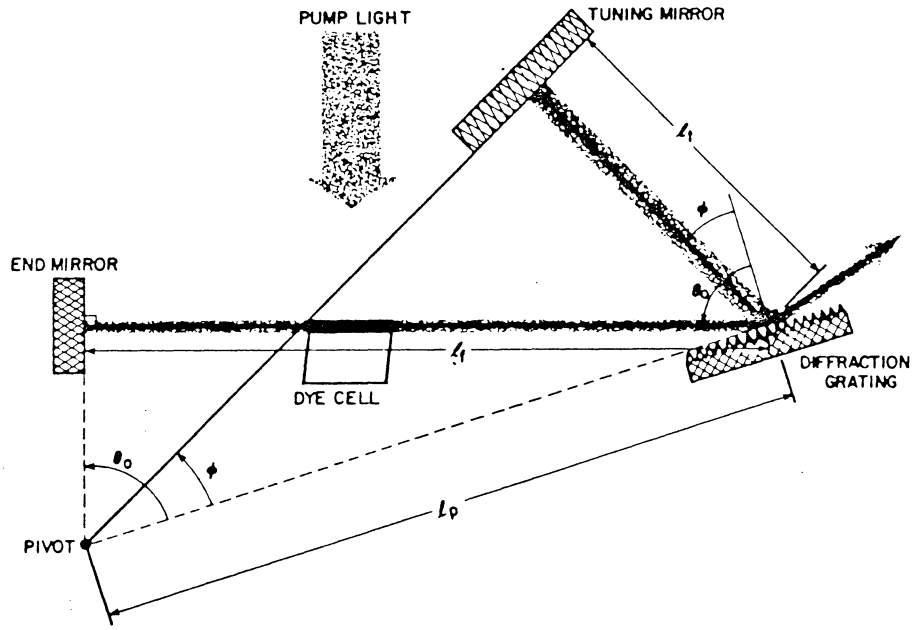

Fig 6.2.1 Grazing incident, pulsed dye laser with self-tracing geometry. (The pivot position as shown is correct, if the optical path length of the dye is equal to its physical length.) [13]

The simplest geometrical solution of the last condition is a right-angled triangle inscribed in a semi-circle as shown in fig 6.2.1 above. The intersection of the largest catheter and the hypotenuse will then be a fixed point in space for all ϕ's and is assumed to be the pivot point. The distance between the middle of the grating and the end mirror is represented by l_f , while l_p represents the distance between the pivot and the middle of the grating and, finally, $l_t(\phi)$ the distance between the tuning mirror and the middle of the grating. Thus the length of the cavity is given by:

$$L(\phi) = l_f + l_t(\phi) \qquad 6.2.3$$

and with

$$l_t(\phi) = l_p \sin \phi \qquad 6.2.4$$

together with 6.2.2 we obtain:

$$N \frac{\lambda}{2} = l_f + l_p \sin\phi. \qquad 6.2.5$$

The wavelength can be expressed by;

$$\lambda = \frac{a}{m}(\sin\Theta_0 + \sin\phi), \qquad 6.2.6$$

from 6.2.1 or by

$$\lambda = \frac{2}{N}(l_f + l_p \sin\phi). \qquad 6.2.7$$

a comparison between equations 6.2.6 and 6.2.7 will result in,

$$l_f = \frac{N\ a}{2\ m} \sin \Theta_o \qquad 6.2.8$$

and

$$l_p = \frac{N\ a}{2\ m}. \qquad 6.2.9$$

At grazing incidence $\sin\Theta_0 \approx 1$ and thus $l_f \approx l_p$, the distance from the middle of the grating to the pivot and from the former to the end mirror coincides. Thus the existence of a pivot point for the tuning mirror with the desired properties is shown, and this point has to be placed in the vicinity of the end mirror, as shown in fig 8.2.1b. In this discussion the index of refraction of the dye and the dye-cell has not been taken into account. The difference in the optical path caused by the dye-cell and the dye will reduce the distance between the end mirror and the grating by about 1 mm.

As the length of the cavity is dependent on the mode number, a change in the length of the cavity of one half wavelength will cause a mode jump. This condition will obviously impose severe requirements on the translation stage. Liu and Littman also found that an error in the position of the end mirror by the order of 0.1 mm will reduce the tuning range from 418 nm to 11 nm [13].

6.3 Homogeneously broadened bands.

The advantage of the short cavity is that it allows multiple passes through the homogeneously broadened laser medium during the time of one pulse of the pump beam. In emission bands of dyes, homogeneously i.e. vibrationally, broadened, each molecule of the dye is capable of contributing its energy at the desired frequency. Thus, when the laser is pumped to well above the threshold of lasing, the broad spontaneous emission is suppressed and most of its emission is concentrated in one frequency. When the active medium is placed in a tuned cavity, stimulated emission can be made to occur at any desired frequency, within the emission bands.

By pumping longitudinally and by focussing the light into a concentrated spot, the gain volume, where the intra-cavity light is forced to interact with the same portion of the active medium on each round trip, will be defined. This will encourage mode competition, resulting in the oscillator running in single mode [12].

7 Developments and applications of the Littman laser

7.1 Developments of the Littman laser

In the original Littman laser design no electronics were considered necessary to control single-mode operations. Experience of operating the original lasers clearly showed that the mechanical tolerance necessary for broad-scan ranges and long, single-mode operations was too rigorous to be attainable. The end-mirror was therefore mounted on a piezo-electric transducer (PZT) permitting fine adjustments of the cavity length. The PZT was complemented with a device to detect the frequency changes of the output light and a feed-back system [15].

7.2 Short-pulse generation

The single-mode Littman oscillator has been used to generate laser pulses with continuously adjustable pulse widths between 0.2 to 3 ns [16], see fig 7.2.1. Rise times shorter than 1 ns are obtained from laser oscillators with a cavity life time shorter than the gain storage time. The efficient cavity length of the Littman oscillator used is about 3 cm, giving a cavity life time of 200 ps, while the gain storage time for DCM in methanol is 1.31 ns. In addition the laser light has a near Fourier transform, limited line width and the laser is tunable in the single-mode. To obtain a short laser pulse, the intensive light from a second dye laser, the quench laser, is directed towards the active region of the Littman oscillator after it has started to oscillate. The quenching light depletes the gain of the Littman oscillator to below the threshold value within the time taken for one single pass.

The Littman oscillator was of the standard type with a 2400 lines/mm grating and a dye cell with a 2 mm optical path. The end mirror was mounted on a PZT which, together with a feed-back system, ensured single-mode operation. The dye was 50 mg/liter DCM in methanol and was pumped with a Nd:YAG laser, the pump light being spatially filtered to produce an Airy-distribution. The light from the Littman oscillator was studied for various values of pump energy. (1, 1.25, 1.6, 2.0 and 2.5 times the threshold energy). Between 1.0 to 2.0 times the threshold energy the laser was running in the single mode, but for 2.5 times the threshold

energy a second mode started to appear.

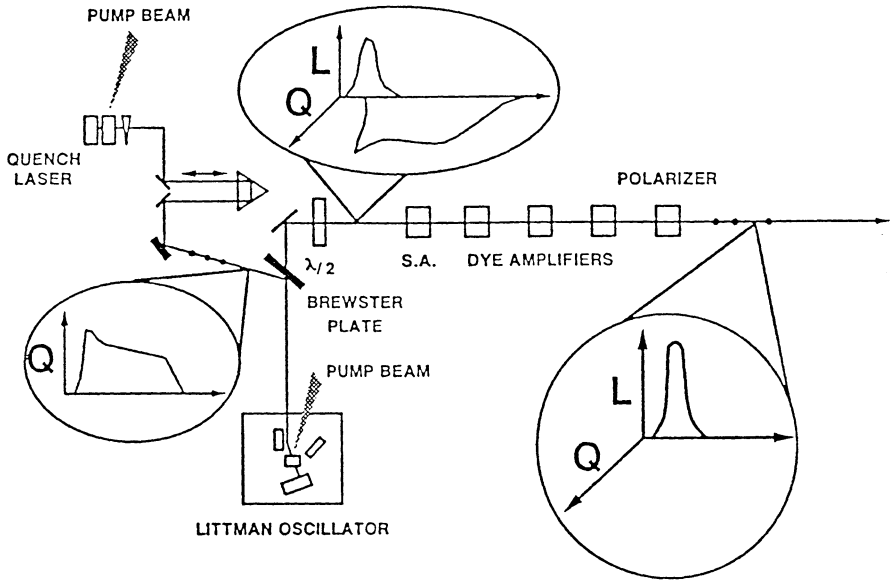

Fig 7.2.1 The dye laser is shown schematically in this figure. The light of the quench laser is reflected from the Brewster plate, quenches the Littman laser oscillator, and is then transmitted, along with the quenched Littman-laser pulse, through the Brewster plate. Both polarization axes are rotated by the Brewster plate for optimum amplification of the Littman laser light. The final polarizer transmits only the light from the Littman laser [16].

The quench laser consisted of a side-pumped dye cell containing DCM, in a 4 cm cavity, consisting of a 100 % reflectance rear mirror and a 4 % reflectance output coupler. It used the same pump laser as the Littman oscillator and is pumped several times above the threshold energy of this laser. The light from the quench laser is directed through a trombone delay line (so called as it resembles the slide of a trombone, see fig 7.2.1 above) and is focused on the active region in the Littman oscillator, using the same lens as the pump light of the Littman oscillator. The length of the output pulse is changed by changing the length of the trombone delay line.

The light from the Littman laser has to be amplified, but this must be done without temporal broadening of the laser pulse, which is manifested

by growth in the tail of the pulse. This will be avoided if the pulse is followed by an orthogonally polarized and sufficiently delayed pulse. The gain recovery in the amplifiers will thus be suppressed. The quench light, which is delayed with respect to the main pulse would, be very suitable for this purpose. The quench pulse is vertically polarized before it enters the delay line, and this light is then directed towards the Littman oscillator by a Brewster plate. With regard to the plate, the light is s-polarized and 15 % of this light is reflected. After quenching, the light is reflected by the end mirror and is both synchronized and orthogonally polarized with respect to the master laser pulse, the latter being p-polarized. Before reaching the amplifier the laser pulse passes through a $\lambda/2$ plate, which rotates the polarization of the pulses. If the Littman laser pulse is polarized parallel to the pump beam the amplification will be three times greater. A saturable absorber will further sharpen the rise time of the Littman laser pulse. The light enters the amplifier section which consists of three amplifier stages. After the amplifier the quench light is removed by a polarizer.

7.3 The Littman cavity with a Ti:Sapphire as active medium.

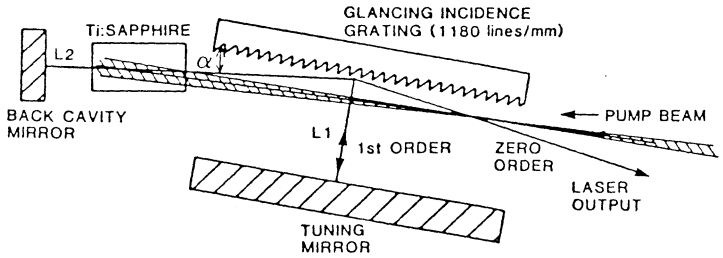

Fig 7.3.1 Components of the SLM (Single- Longitud i n al- Mode laser), tunable, Ti:Sapphire oscillator. The cavity length is $L_1 + L_2$, where L_1 is the distance from the grating to the tuning mirror and L_2 is the distance from the grating to the back mirror [17].

A new and interesting design based on the Littman oscillator, is one in which the dye cell has been replaced by block of a solid state Ti:Sapphire [17]. The new oscillator runs in single longitudinal mode, the energy of its output pulse is 2 to 3 orders of magnitude greater than

a conventional Littman design, it has an output beam quality of TEM_{oo} and is tunable from 746 to 918 nm. The correct pivot point of the tuning mirror has not been chosen with the result that mode hops occurred during tuning. However, synchronous tuning without mode hops is possible when this pivot point is located. The design is shown in fig 7.3.1 above.

8 Experiments with the Littman laser.

8.1 The experimental arrangement.

The Littman cavity, essentially a simple, compact design, consists of two mirrors, one grating and one dye cell, contained within an area of 1 dm^2. A prerequisite for lasing is that the components must be arranged according to the geometrical conditions discussed in the previous chapter and, if single-mode tuning is required, the pivot must be determined with high precision. At the base of the dye laser, the tuning mirror is allowed to rotate around a certain fixed point, the pivot, and the other components of the laser must be arranged according to the geometrical conditions of this laser, without changes in the cavity length greater than $\lambda/2$.

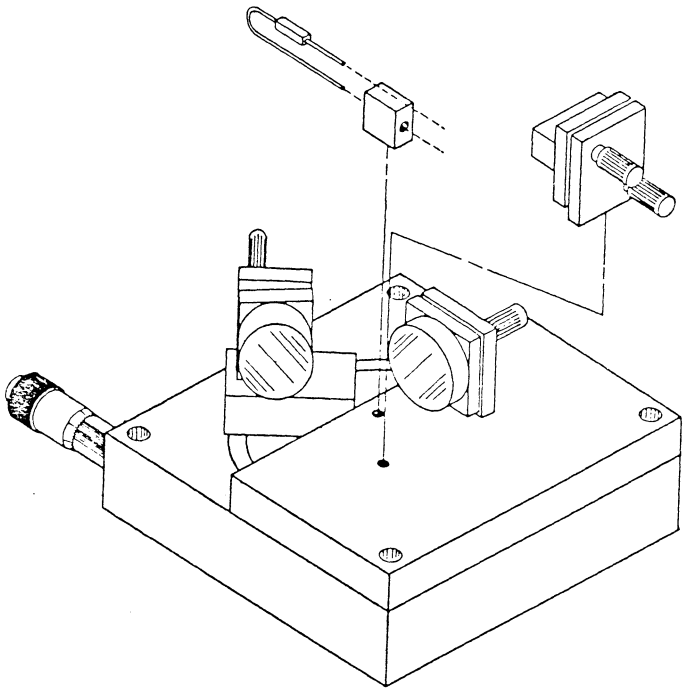

Fig 8.1.1 Exploded view of a single-mode, pulsed, tunable, dye laser [18].

As a base a high resolution stage is used which provides a fine adjustment of wobble-free angular motion over 16^o travel. To obtain a resolution of 0.3 arcsec a differential micrometer is used. The mounting of the tuning mirror is rigidly attached to a pedestal bolted to the rotational stage. A metal plate, providing a base for attaching the other

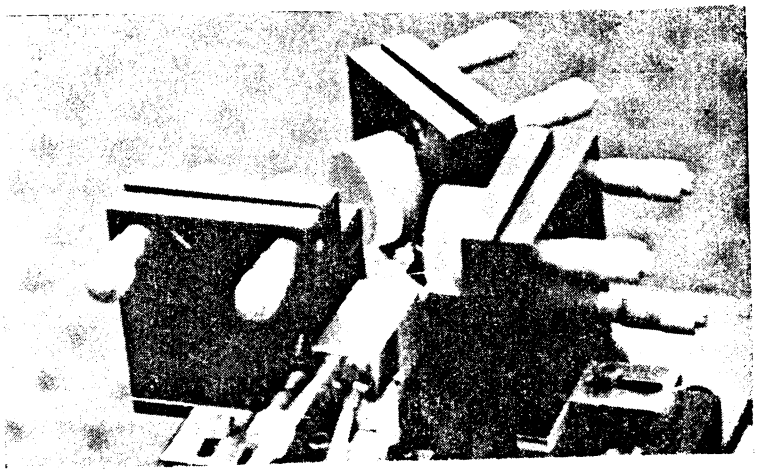

Fig 8.1.3 The Littman cavity, viewed from behind.

8.2 The Alignment

As ASE (Amplified Spontaneous Emission) is very weak for this kind of laser, it is impossible to align the optical components by this light only. The use of a HeNe laser is thus necessary for this purpose [16]. A triangular gauge of soft card board is made to be used for the positioning of the optical components. The direction of the alignment beam is opposite to the of the dye-laser beam. When it strikes the grating at an angle of incidence of about 89^{o}, the diffracted light of the first order is clearly seen at an angle of refraction of about 31^{o}. The spot is long, narrow and very bright.

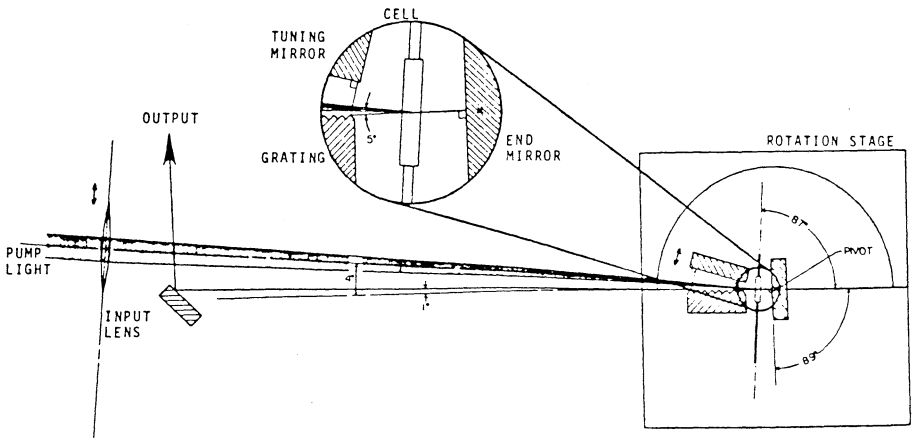

Fig 8.2.1 The laser seen from above showing the relative positions of the beams [18].

the laser. Note, if the laser is to operate well, the alignment beam from the HeNe laser and the pump beam are in the same plane.

To identify the intra-cavity and extra-cavity optic axis as well as aiding in the pitch adjustment of the tuning mirror, a microscopic slide is used to set up lasing with the end mirror, using the grating reflection off the diffraction grating. Once the laser is oscillating the microscope slide is removed. A way to check whether the laser is oscillating properly when using the slide, is to observe the zero order reflection of the grating from the tuning mirror. If the laser is oscillating in a proper way the spot will be very diffuse.

8.3 Experiments

For this diploma work basically two types of experimental arrangements were used. These will be briefly discussed here.

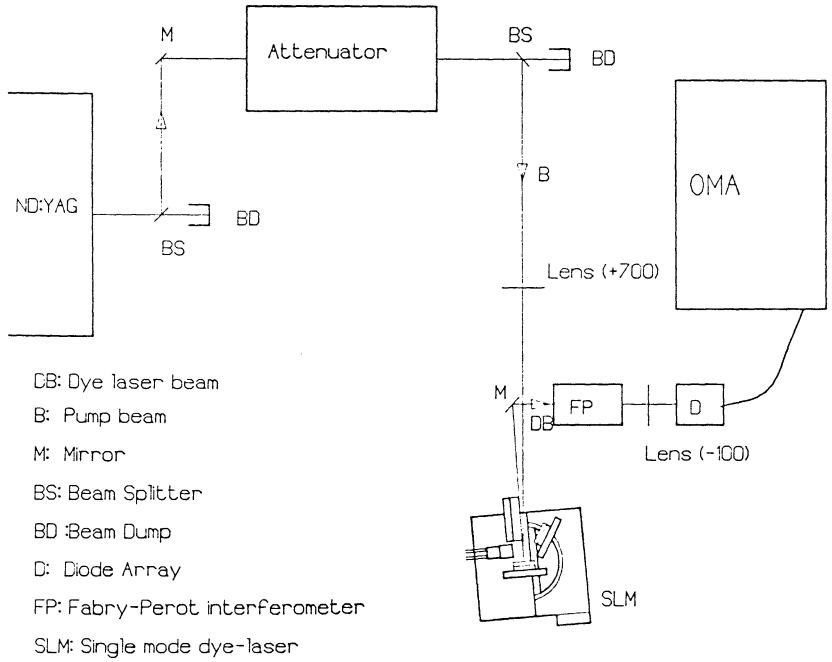

Fig 8.3.1 The set-up 1

In the second set-up the goal was to eliminate glass in the pump beam and to replace mirrors by prisms. In the first set-up, the intensity of the pump light was continuously attenuated. The attenuator used was replaced by neutral density filters in the second set-up.

and because of severe alignment difficulties.

The spectra were recorded by an OMA III diode-array detector in the first and a TRACOR Northern diode-array detector in the second set-up. With a dye concentration of $4 \cdot 10^{-4}$ M, the laser performed well. The intensity of the beam fluctuated from shot to shot but even the lowest intensity was well above threshold. When the laser was not adjusted for lasing, this did occur between the front and the end walls of the dye cell. When the dye laser was operating no such lasing was observed, but a laser beam in the vertical direction indicated lasing between the upper and lower walls of the dye cell.

When observed on a screen placed in front of the dye laser the beam appeared as a bright, almost circular, spot consisting of a bright inner spot surrounded by a circular area of lower intensity. At a concentration of $4 \cdot 10^{-4}$ and with a pump energy of 1 mJ the angular spread was 2.88 mrad. Under the same conditions the tuning range was determined. The tuning mirror was rotated between the points at which the laser started to run and these points were fixed. The tuning range was 608 to 643 nm, an interval of 35 nm. It was impossible to determine the mode structure at this time as the 7.5 GHz interferometer was broken.

To investigate the effect of the polarization of the pump beam on the intensity of the dye laser beam a tunable $\lambda/4$ plate was placed in the pump beam. The output was studied with a photo diode and an oscilloscope.

The performance of the dye laser was studied at several concentrations of the dye. These ranged from $8 \cdot 10^{-4}$ M to $2 \cdot 10^{-4}$ M. The pump energies ranged from 1.75 mJ to 0.5 mJ in steps of 0.25 mJ. On some occasions even 1.9 mJ was used. Higher energies were avoided so as not to risk damage the dye cell.

The laser performed well in this range of concentrations but it was difficult to initiate lasing for concentrations below $4 \cdot 10^{-4}$ M. At a concentration of $2 \cdot 10^{-4}$ M it was very difficult to make the laser run. An attempt was made to make the laser run with concentrations of $1.5 \cdot 10^{-4}$ M

and $1.0 \cdot 10^{-4}$ M but with negative results. At a concentration of $8 \cdot 10^{-4}$ M the laser started to run readily. Even at $4 \cdot 10^{-4}$ M the laser was running without any great difficulties, but to reach concentrations below this, it is recommended to start with a high concentration and carefully dilute the dye until the desired concentration is reached. Some adjustments of the cavity might be necessary during the process. This operation should be monitored with spectroscopic equipment.

For concentrations of $4 \cdot 10^{-4}$ M and higher the pump energy threshold was below 0.5 mJ, but at concentrations of $3.0 \cdot 10^{-4}$ M and $2 \cdot 10^{-4}$ M the threshold increased to about 0.70 mJ and 1.0 mJ.

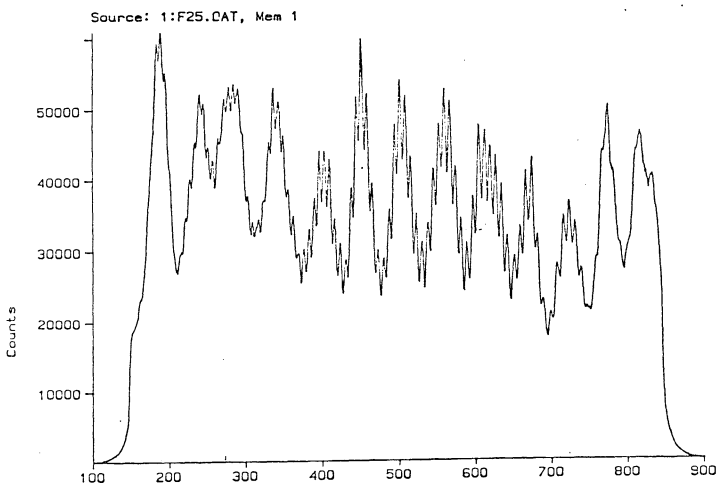

Fig 8.3.3 Pattern from Littman laser, obtained by 1.5GHz fsr Fabry-Perot confocal interferometer.

a) E_p = 1.7 mJ, 0.4 mM DCM in methanol.

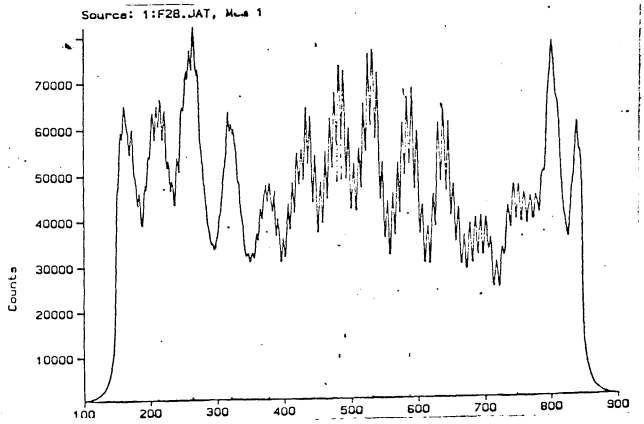

b) E_p = 1.0 mJ, 0.4 mM DCM in methanol.